Inhibitory effect of PDE2 on inflammation and apoptosis in cerebral ischemia-reperfusion injury

DING WAN[1,2], XIAOYAN WANG[3], JIN FENG[1], PENG WANG[2] and HUA XU[4]

[1]Department of Neurosurgery, General Hospital of Ningxia Medical University;
[2]Ningxia Key Laboratory of Cerebro Cranial Disease, Ningxia Medical University, Yinchuan, Ningxia 750004;
[3]Department of Hospital Infection Management, Zhongning County People's Hospital, Zhongwei, Ningxia 751200;
[4]Department of Nursing, Wuxi Higher Health Vocational Technology School, Wuxi, Jiangsu 214028, P.R. China

Abstract. Cerebral ischemia-reperfusion injury (CIRI) is associated with high morbidity and mortality rates and its pathogenesis is complex. Phosphodiesterase 2 (PDE2) has been proposed to exert a protective effect, although, to the to the best of the authors' knowledge, its role in CIRI has yet to be reported. Therefore, the aim of the present study was to investigate the role of PDE2 in CIRI. To meet this aim, a middle cerebral artery occlusion (MCAO) model was established in mice. After having successfully modeled the MCAO, the mice were treated with the PDE2 inhibitor Bay-607550 and the expression level of PDE2 was detected using reverse transcription-quantitative (RT-q) PCR and western blot analysis. Histopathology of the brain was assessed using hematoxylin and eosin staining. The proportions of dry and wet tissue in brain were recorded and the cerebral ischemia area was assessed using 2,3,5-triphenyltetrazolium chloride staining. RT-qPCR was also used to measure the expression levels of inflammatory factors. The expression of ionized calcium binding adaptor molecule 1, a marker of microglia activation, was detected by immunofluorescence assay, western blotting and RT-qPCR. Western blotting was used to detect the expression levels of P65 and NF-κB inhibitor α and their phosphorylated forms. The levels of apoptosis were subsequently determined using TUNEL and western blot analysis. SH-SY5Y cells were induced by oxygen-glucose deprivation (OGD) and the expression levels of PDE2 were subsequently detected. Cell transfection was used to interfere with the expression of PDE2 and the regulation of PDE2 upon OGD/reoxygenation (OGD/R)-induced inflammation and apoptosis was further detected in cell experiments. Finally, western blot analysis was used to detect the expression of protein kinase A (PKA) downstream of PDE2 *in vivo* and *in vitro*. The expression levels of PDE2 were found to be significantly increased in the MCAO model mice. Following treatment with Bay-607550, the condition of the brain nerve cells was improved with respect to the levels of cerebral ischemia, inflammation and apoptosis. The results of the *in vitro* cell experiments were found to be consistent with those of the *in vivo* animal experiments. Furthermore, the western blotting experiments suggested that the above-mentioned regulation of PDE2 may be achieved via regulating PKA. Taken together, the present study has shown that inhibition of PDE2 led to a reduction in inflammation and apoptosis during CIRI through regulating PKA.

Introduction

Cerebral ischemia is caused by blood vessel blockage, resulting in reduced cerebral blood flow and brain damage. The longer that the decrease in cerebral blood flow lasts, the more severe is the brain damage that occurs (1). Reperfusion of blood flow in ischemic areas can also cause brain tissue damage and associated dysfunction and this process is termed cerebral ischemia-reperfusion injury (CIRI) (2). CIRI is characterized by high morbidity, high disability and high mortality rates (3) and the timely restoration of blood-flow reperfusion in the ischemic area is the primary treatment method for this type of disease. However, the mechanism of CIRI is complex and the aim of the present study was to gain further insights into the pathogenesis of CIRI.

Phosphodiesterase (PDEs) are metal-dependent phosphohydrolases that metabolize the second messenger cyclic adenosine phosphate (cAMP) and cyclic guanosine phosphate (cGMP) into their respective inactive 5'-phosphates (4). PDEs are subdivided into 11 structurally related, but functionally distinct families (PDE1-11) based on different post-translational modifications and cyclic nucleotide substrates (5). In general, PDEs are involved in numerous physiological processes, including cell proliferation and differentiation, gene expression, inflammation, apoptosis and metabolism (6). The isozyme PDE2, as a member of the PDE family, is mainly distributed in the central nervous system of the human body

Correspondence to: Dr Hua Xu, Department of Nursing, Wuxi Higher Health Vocational Technology School, 305 Xinguang Road, Wuxi, Jiangsu 214028, P.R. China
E-mail: xuhuachong2021@163.com

and is highly expressed in the cerebral cortex and hippo-campus (7). Previous studies have shown that PDE2 inhibitors are able to inhibit PDE2 protein activity, thereby increasing the levels of cAMP and cGMP and enhancing long-term synaptic transmission and ultimately improving cognitive and memory functions in patients with Alzheimer's disease and aging brain populations (8,9). In addition, the PDE2 inhibitor Bay 60-7550 has been demonstrated to ameliorate Aβ-induced cognitive and memory impairment in mice through regulating the hypothalamic-pituitary-adrenal axis, or HPA axis (10). Moreover, the novel PDE2 inhibitor Hcyb1 is shown to produce neuroprotective and antidepressant-like effects, probably mediated through the cAMP/cGMP-CREB-BDNF signaling axis (11). However, it remains to be elucidated whether PDE2 is able to inhibit neuroinflammation and neuronal apoptosis during CIRI.

Therefore, the aim of the present study was to explore the role of PDE2 in CIRI and the underlying mechanism(s) through *in vivo* and *in vitro* experiments. The results obtained provided a theoretical basis for the treatment of CIRI.

Materials and methods

Establishment of the middle cerebral artery occlusion (MCAO) model. Male C57BL/6J mice (n=15; 8 weeks old; 18-22 g) provided by Department of Laboratory Animal Science, Peking University Health Science Center were housed in an environment with 50±10% humidity, constant (25°C) tempera-ture with regular 12-h light/dark cycle and given *ad libitum* access to water and food for 1 week prior to modeling. Mice were then randomly divided into the control group, the MCAO group and the MCAO + Bay-607550 group; for the latter group, the mice were treated with Bay-607550 (cat. no. 439083-90-6; Merck KGaA), an inhibitor of PDE2. Each group contained five mice. Mice in the MCAO + Bay-607550 group were administered Bay-607550 (1 mg/kg/day) by gavage for 14 days. Subsequently, all mice were anesthetized with sodium pentobarbital (40 mg/kg, intraperitoneal injection) and in the MCAO and MCAO + Bay-607550 groups, a midline incision in the neck was made to expose the right common carotid artery along with the vagus nerve, followed by blunt dissection of the internal carotid artery, together with the external carotid artery. Focal cerebral ischemia was then induced by the occlu-sion of the MCA with a nylon fishing line (0.38 mm diameter) for 2 h. The filament was removed 1 h after MCA occlusion and reperfusion was allowed to proceed for 24 h. Mice in the control group underwent the same procedure, but without the filament insertion procedure. After successful modeling, the mice were sacrificed by cervical dislocation (mortality was confirmed when the mice stopped breathing, their hearts stopped beating, their muscles relaxed, their body temperature dropped and they did not respond to external stimuli). All these animal experiments were approved by the ethics committee of Wuxi Higher Health Vocational Technology School and the NIH Guide for the Care and Use of Laboratory Animals, 8th (grants.nih.gov/grants/olaw/Guide-for-the-Care-and-use-of-laboratory-animals.pdf) was followed rigorously.

Reverse transcription-quantitative (RT-q)PCR. Total RNA was extracted from samples which are inoculated into 6-well plates at a density of $1x10^3$ cells/well using TRIzol® (Thermo Fisher Scientific, Inc.) from cells or brain tissues according to the manufacturer's protocols. cDNA synthesis from 1 μg total RNA in a reaction volume of 20 μl was performed using the miScript SYBR® Green PCR kit (DBI Bioscience) according to the manufacturer's protocols. The amplification was performed using Real-time PCR Detection System (Mx3000P qPCR system; Agilent Technologies, Inc.) according to the manufacture's protocol. Each experiment was replicated three times. The relative RNA expression levels were quantified using the $2^{-\Delta\Delta Cq}$ method (12). GAPDH was used as the control RNA species. The primer sequences used were as follows: mice: PDE2 forward, 5'-CAGACTGGTGTG TGAGGACC-3' and reverse, 5'-ACGTGTTCATCCTCATCT GTGA-3'; TNF-α forward, 5'-TCCTCACCCACACCGTCA G-3' and reverse, 5'-GCTGAGTTGGTCCCCCTTC-3'; IL-1β forward, 5'-TTCTCGCAGCAGCACATC-3' and reverse, 5'-CAGCAGGTTATCATCATCATCC-3'; IL-6 forward, 5'-TCCATCCAGTTGCCTTCTT-3' and reverse, 5'-TTTCTC ATTTCCACGATTTCC-3'; MCP-1(CCL2) forward, 5'-CTG TTCACAGTTGCCGGCTG-3' and reverse, 5'-AGCTTCTTT GGGACACCTGCT-3'; Iba-1(AIF1) forward, 5'-TGAGGA GATTTCAACAGAAGCTGA-3' and reverse, 5'-CCTCAG ACGCTGGTTGTCTT-3'; and GAPDH forward, 5'-CCC TTAAGAGGGATGCTGCC-3' and reverse, 5'-ACTGTG CCGTTGAATTTGCC-3'. Human: PDE2 forward, 5'-CAC CACATCCTCATCGCTGT-3' and reverse, 5'-AGGCAT CCAGGTCGTAGAGT-3'; TNF-α forward, 5'-CTGGGC AGGTCTACTTTGGG-3' and reverse, 5'-CTGGAGGCC CCAGTTTGAAT-3'; IL-1β forward, 5'-AGCCATGGC AGAAGTACCTG-3' and reverse, 5'-TGAAGCCCTTGC TGTAGTGG-3'; IL-6 forward, 5'-GTCCAGTTGCCTTCT CCCTGG-3' and reverse, 5'-CCCATGCTACATTTGCCG AAG-3'; MCP-1 forward, 5'-GATCTCAGTGCAGAGGCT CG-3' and reverse, 5'-TTTGCTTGTCCAGGTGGTCC-3'; Iba-1 forward, 5'-CTCCAGCTTGGAGGAAAAGC-3' and reverse, 5'-TGGAGGGCAGATCCTCATCA-3'; and GAPDH forward, 5'-AATGGGCAGCCGTTAGGAAA-3' and reverse, 5'-GCGCCCAATACGACCAAATC-3'.

Western blot analysis. RIPA lysate (Thermo Fisher Scientific, Inc.) was added to SH-SY5Y cells and brain tissues to extract the proteins, following the manufacturer's protocol. A BCA protein assay kit (Beyotime Institute of Biotechnology) was used to determine the protein concentration. The proteins (20 μg per lane) were separated using SDS-PAGE (10% gels) and subsequently transferred to PVDF membranes (Bio-Rad Laboratories, Inc.) which were blocked by 5% non-fat milk for 2 h at room temperature. The membrane was incubated with the corresponding primary antibody PDE2 (1:1,000; cat. no. ab271673); Iba-1 (1:1,000; cat. no. ab178846); p-p65 (1:1,000; cat. no. ab76302); p65 (1:1,000; cat. no. ab76311); p-IkB-α (1:1,000; cat. no. ab133462); IkB-α (1:1,000; cat. no. ab32518); Bax (1:1,000; cat. no. ab32503); cleaved caspase3 (1:1,000; cat. no. ab214430); caspase3 (1:1,000; cat. no. ab184787); cleaved PARP (1:1,000; cat. no. ab32064); PARP (1:1,000; cat. no. ab191217); PKA (1:1,000; cat. no. ab32390) and GAPDH (1:1,000; cat. no. ab8245) all from Abcam, overnight at 4°C. The following day, the Goat Anti-Mouse IgG H&L (Alexa Fluor 647; 1:5,000; cat. no. ab150115, Abcam) was incubated

with the membranes at room temperature for 2 h. The protein bands were visualized using chemiluminescence (ECL; Merck KGaA) assay and the blots were semi-quantified using ImageJ software (version 146; National Institutes of Health).

Hematoxylin and eosin (H&E) staining. Brain tissues of mice were isolated and fixed in 10% formalin (Beyotime Institute of Biotechnology) at room temperature for 24 h. The tissues were dehydrated with 90% ethanol for 2 min and embedded with paraffin for 5 min and then cut into 5-μm-thick sections for H&E staining.

Neurological score. Behavioral tests were performed at 3 days after reperfusion. The five-point scale was as follows: 0, no neurological deficits; 1, failure to extend the contralateral forepaw fully; 2, circling to the ipsilateral side when held by the tail; 3, falling to the contralateral side; and 4, did not walk spontaneously and had a reduced level of consciousness. Higher neurological deficit scores indicated more severe impairment of motor injury.

Brain water (BW) content. The two hemispheres were evaluated on an electronic balance for wet weight and subsequently dried in an oven for 24 h at 100˚C for determination of the dry weight. BW was calculated as follows: BW = (wet weight-dry weight)/wet weight x100%.

2,3,5-Triphenyltertrazolium chloride (TTC) staining. The brain sections were incubated in 2% TTC phosphate buffer (pH 7.4) for 30 min at 37˚C and subsequently fixed with 10% formaldehyde solution for 24 h to enhance the color contrast. Cerebral sections were assessed for the observed levels of ischemia and unstained areas were measured with ImageJ software (Version 146; National Institutes of Health) to calculate the percentage of grayish-white areas. The white parts represented ischemic areas.

Immunofluorescence (IF) analysis. Brain slices (20 μm) were fixed with 4% paraformaldehyde for 15 min at room temperature and then separately permeabilized with 0.5% Triton X-100 in PBS for 10 min at room temperature. After the slices had been blocked with 2% BSA for 2 h at room temperature, they were stained with anti-IBA1 antibody (1:200; cat. no. GT10312, Thermo Fisher Scientific, Inc.) for 1 h at 37˚C. Subsequently, brain slices were incubated with goat anti-mouse secondary antibody (1 μg/ml; cat. no. A-11001, Invitrogen; Thermo Fisher Scientific, Inc.) for 1 h at 37˚C. Finally, the brain slices were stained with 100 nM DAPI (MilliporeSigma) for 15 min at room temperature and samples were observed under a fluorescence microscope (Zeiss GmbH).

TUNEL analysis. A One Step TUNEL Apoptosis Assay kit (Beyotime Institute of Biotechnology) was used to assess the extent of apoptosis, according to the manufacturer's instructions. Transfected cells were fixed using 4% paraformaldehyde for 1 h at 4˚C and then 0.1% Triton X-100 was added at room temperature for 5 min. Cells were washed with PBS and incubated with TUNEL reagent for 1 h at 37˚C. Then, 50 μl DAB color development was performed for 10 min at 15˚C according to the manufacturer's instructions. The cells were stained with DAPI for 10 min at room temperature in the dark. Stained cells were observed under a glass coverslip with PBS using a fluorescent microscope (magnification, x200; Carl Zeiss AG). Subsequently, a fluorescence microscope (Nikon Corporation) was used to capture images of the cells and to count the TUNEL-positive cells. ImageJ software (Version 1.8.0; National Institutes of Health) was used to count the total cells and the TUNEL^{+} cells. The number of apoptotic cells was calculated to be the average number of positive cells out of the total number of cells in six fields of view per slide.

Cell culture. SH-SY5Y cells obtained from Cell Bank of the Chinese Academy of Sciences were cultured in DMEM supplemented with 10% FBS and 100 U/ml penicillin (all from Gibco; Thermo Fisher Scientific, Inc.) at 37˚C in an atmosphere of 5% CO_2. STR profiling was carried out in order to verify the authenticity of the SH-SY5Y cell line.

Oxygen-glucose deprivation (OGD) and reoxygenation (OGD/R). SH-SY5Y cells were cultured in Hank's Balanced Salt Solution (HBSS; Merck KGaA) and then incubated with a gaseous mixture of 5% CO_2/95% N_2 for 60 min at 37˚C. The OGD treatment was stopped by replacing HBSS with 15% FBS. The cells were then returned to normoxic conditions for 24 h for re-oxygenation. Control culture cells were incubated with the HBSS buffer supplemented with 15 mM glucose in a humidified incubator under normoxic conditions for the same period of time as the OGD cultures. The control cells group was treated the same as the OGD/R group, with the exception that the culture gas was different. Cells were pretreated with 1 μM Bay-607550 for 30 min.

Cell transfection. Small interfering (si) RNAs for PDE2 (siRNA-PDE2-1 and siRNA-PDE2-2) or siRNA negative control (siRNA-NC) were synthesized by Guangzhou RiboBio Co., Ltd. and transfections into the SH-SY5Y cells at 20 nM were performed with Lipofectamine 2000® reagent (Invitrogen; Thermo Fisher Scientific, Inc.) at room temperature for 20 min. Cells were harvested at 48 h after the transfection for further study. si-PDE2-1: sense 5'-AUAUUG AAGGACUUUGAGCUG-3', antisense 5'-GCUCAAAGU CCUUCAAUAUCU-3'; si-PDE2-2: sense 5'-UAUGAUACA UCAUCAUCUCAU-3', antisense 5'-GAGAUGAUGAUGUAU CAUAUG-3'; si-NC: sense 5'-GACGUAAACGGCCACAAG UUC-3', antisense 5'-ACUUGUGGCCGUUUACGUCGC-3'.

Statistical analysis. Data were analyzed with GraphPad Prism version 8.0 (GraphPad Software, Inc.) and expressed as the mean ± SD. Comparisons among multiple groups were performed with one-way ANOVA followed by a Tukey's post hoc test. The neurological scores were presented as median and IQR, and statistically analyzed using Kruskal-Wallis and Dunn's post hoc test. $P<0.05$ was considered to indicate a statistically significant difference.

Results

A PDE2 inhibitor, Bay-607550, reduces histopathological damage in CIRI tissue. The expression of PDE2 in mouse brain tissues was detected using RT-qPCR and western blot analysis.
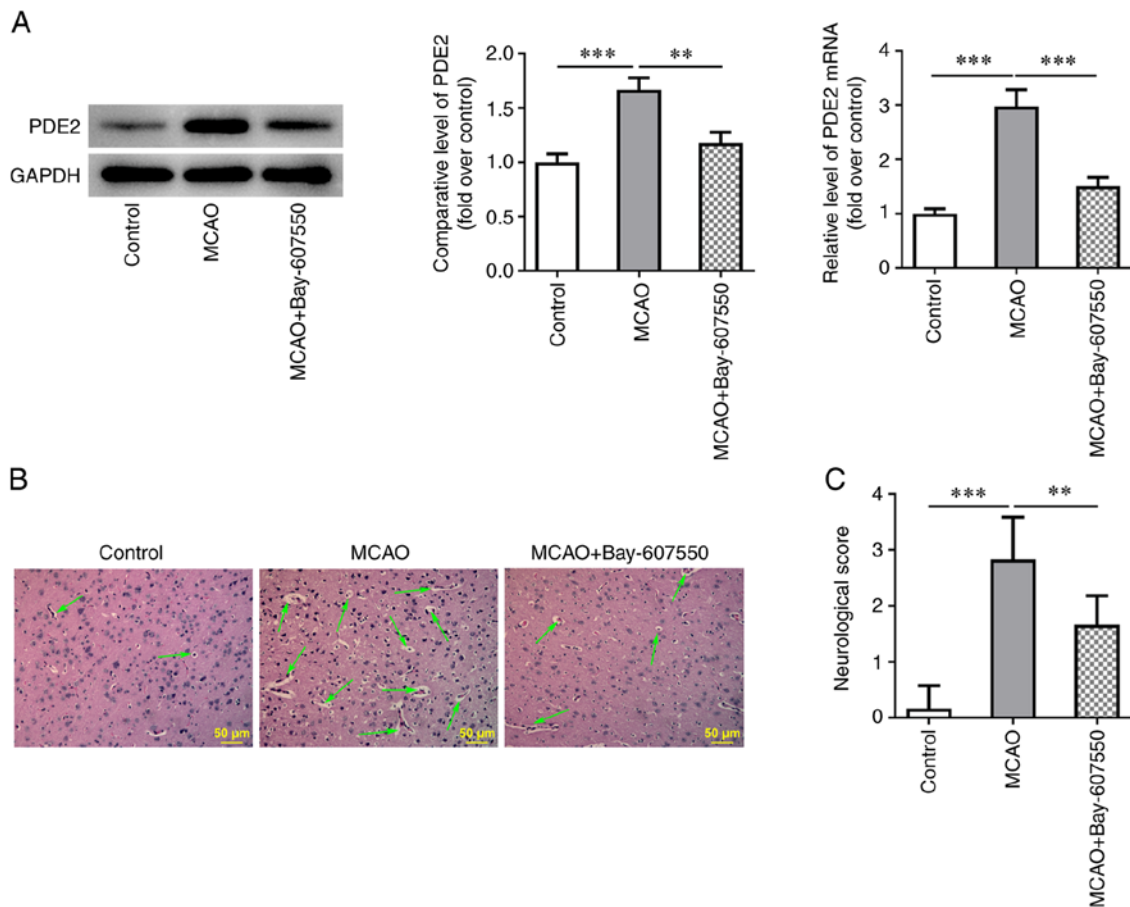
Figure 1. PDE2 inhibitor reduces histopathological damage in CIRI tissues. (A) Western blotting and reverse transcription-quantitative PCR detected the expression of PDE2. (B) Hematoxylin and eosin staining detected the pathological changes of cerebral ischemia tissue. The arrows indicate the shrinkage of nerve cells and the edema of tissue. (C) Neurological function score was used to judge the neurological function of mice. **$P<0.01$, ***$P<0.001$. PDE, phosphodiesterase; CIRI, cerebral ischemia-reperfusion injury.
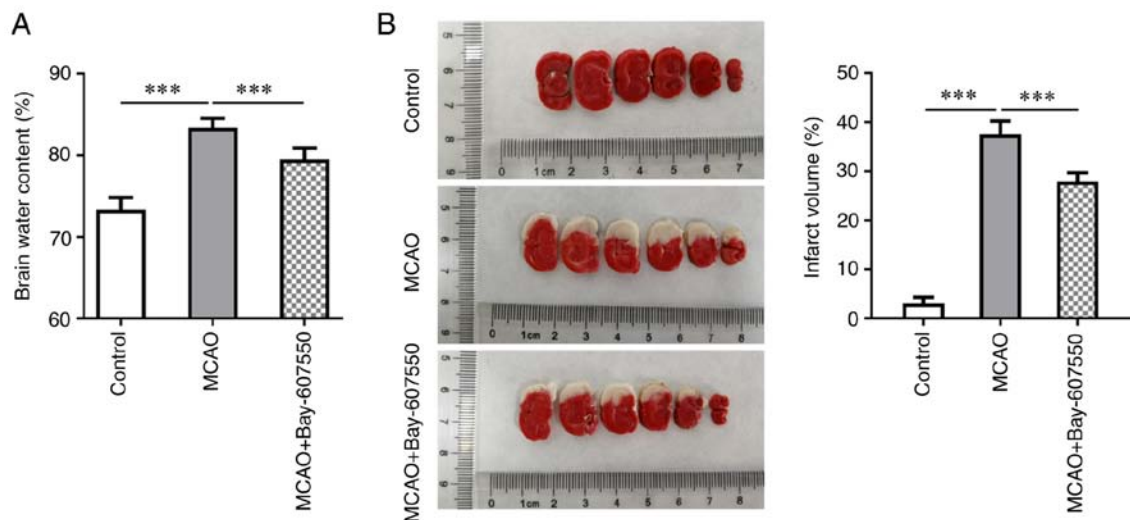

Figure 2. PDE2 inhibitor reduced cerebral edema and ischemic area in CIRI mice. (A) The dry weight/wet weight ratio was recorded to observe the cerebral edema of mice. (B) Cerebral ischemia area was detected by 2,3,5-Triphenyltertrazolium chloride staining. ***$P<0.001$. PDE, phosphodiesterase; CIRI, cerebral ischemia-reperfusion injury.

The results obtained showed that the expression of PDE2 was significantly increased in the MCAO group compared with the control group. By contrast, the increases in PDE2 expression were reversed after treatment with the PDE2 inhibitor, Bay-607550, compared with the MACO group (Fig. 1A). Histopathological damage was subsequently detected by H&E staining. The results obtained showed that the histopathological damage of mice in the MCAO group was severe. However,
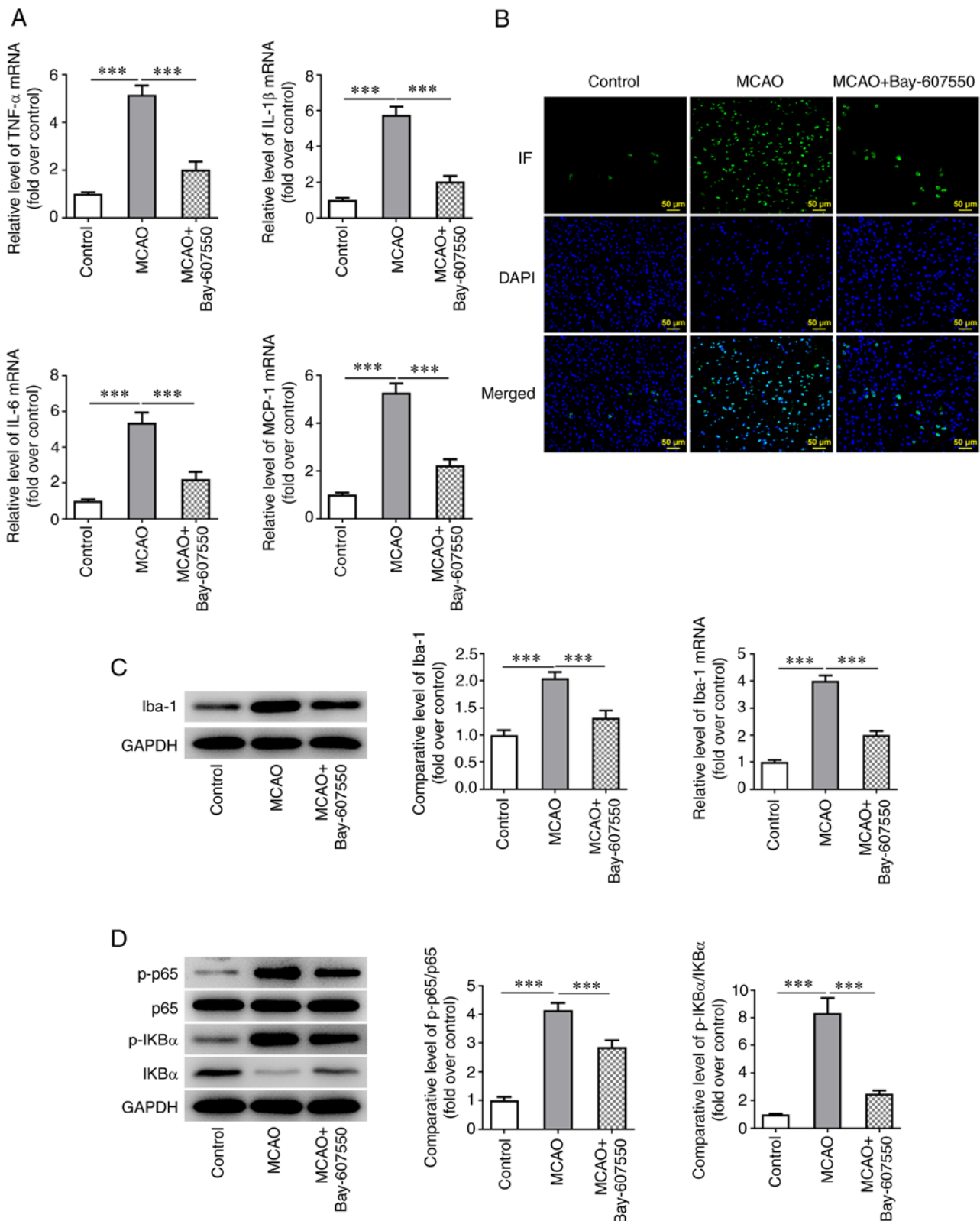
Figure 3. PDE2 inhibitor reduces inflammatory and the activation of microglia in CIRI mice. (A) RT-qPCR detected the expression of TNF-α, IL-1β, IL-6 and MCP-1. (B) The expression of Iba was detected by IF staining. (C) The expression of Iba was detected by western blotting and RT-qPCR. (D) Western blotting was used to detect the expression of p-P65, p-IkB-α, P65 and IkB-α. ***P<0.001. PDE, phosphodiesterase; CIRI, cerebral ischemia-reperfusion injury; RT-qPCR, reverse transcription-quantitative PCR; TNF, tumor necrosis factor; IL, interleukin; MCP, monocyte chemoattractant protein; Iba, ionized calcium binding adaptor; IF, Immunofluorescence; p-, phosphorylated; IkB-α, NF-κB inhibitor α.

after the MCAO-modeled mice were treated with Bay-607550, the histopathological damage of brain tissue was found to be significantly ameliorated (Fig. 1B). The neurological function of the mice was then scored and this analysis revealed that the MCAO group experienced the highest and most severe neurological injury scores compared with the control group.
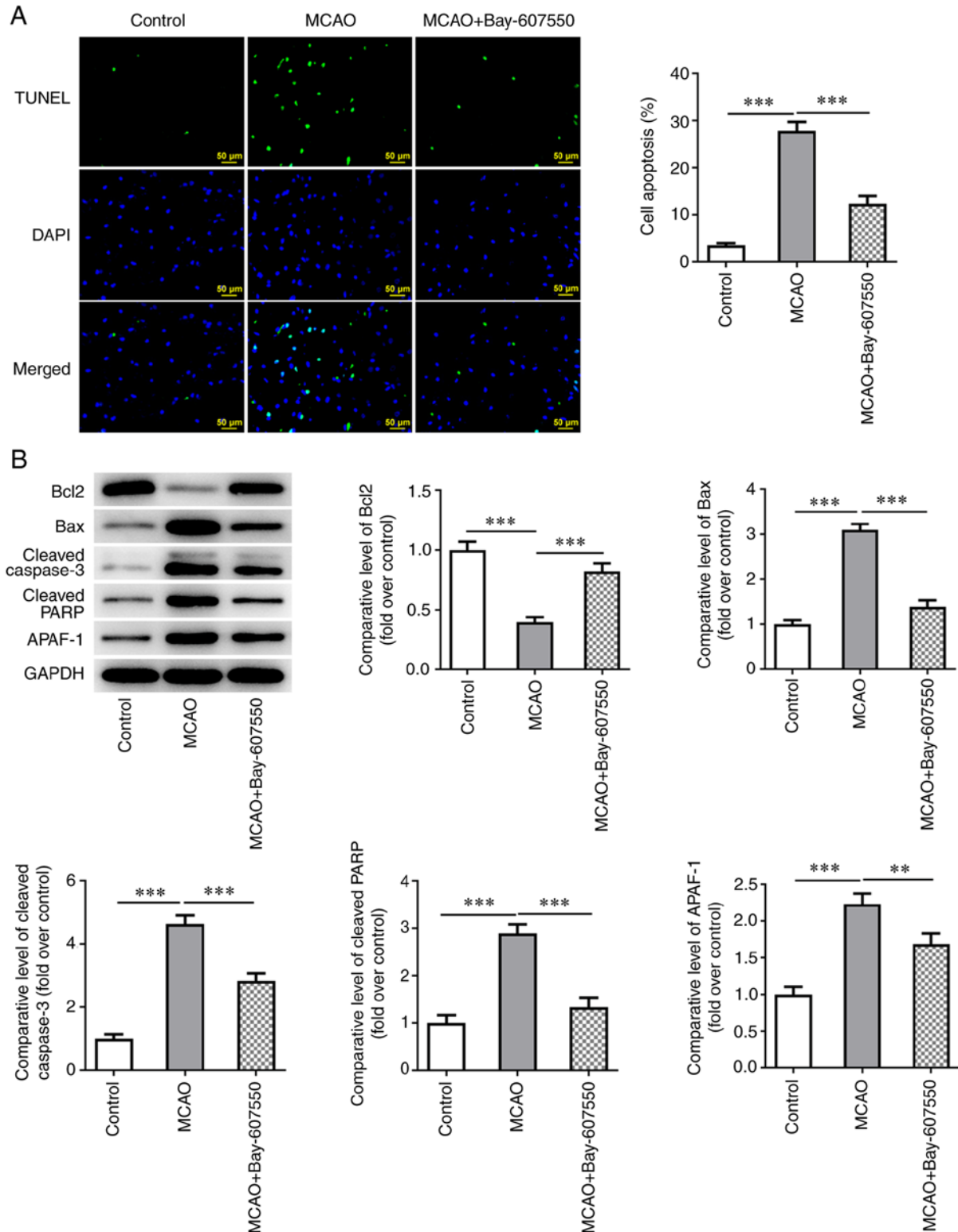
Figure 4. PDE2 inhibitor reduced the apoptosis of nerve cells in CIRI mice. (A) TUNEL assay detected the apoptosis of brain tissue cell. (B) Western blotting was used to detect the expression of apoptosis-related proteins. **P<0.01, ***P<0.001. PDE, phosphodiesterase; CIRI, cerebral ischemia-reperfusion injury.

However, compared with the MCAO group, the MCAO + Bay-607550 group did not have such pronounced neurological injury scores (Fig. 1C).

The PDE2 inhibitor Bay-607550 reduces cerebral edema and ischemic area in CIRI mice. Subsequently, the dry weight/wet weight ratio of the mice was measured in order to observe the cerebral edema of mice. These results showed that cerebral edema in the MCAO group was more severe compared with the control group. Furthermore, compared with the MCAO group, cerebral edema was significantly improved in the MCAO + Bay-607550 group (Fig. 2A). Subsequently, TTC staining was used to detect cerebral ischemia. These results are shown in Fig. 2B; specifically, no clear cerebral ischemia
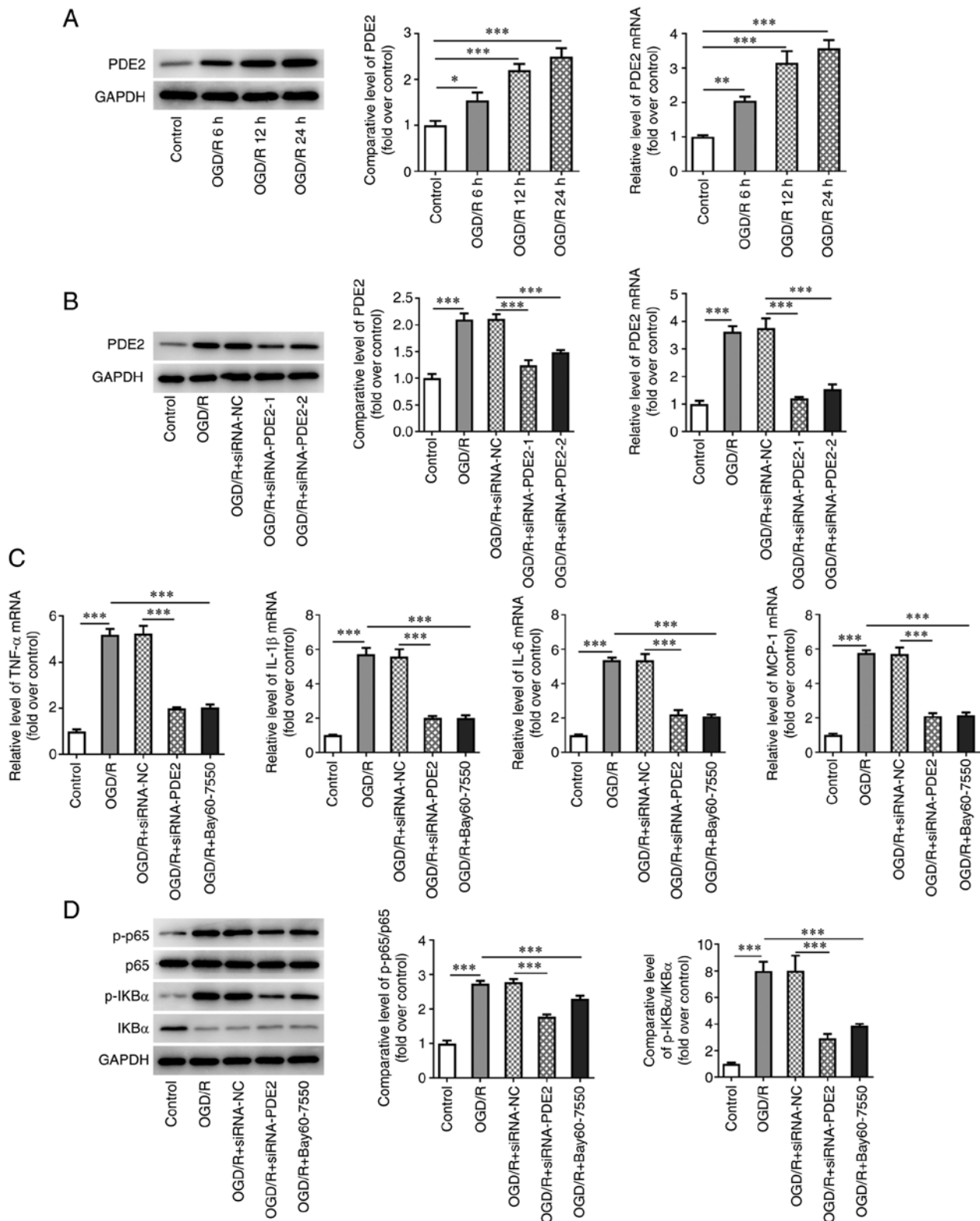
Figure 5. PDE2 inhibitor reduced OGD/R induced neuronal inflammation. (A) Western blotting and RT-qPCR detected the expression of PDE2 in OGD/R induced SH-SY5Y cells. (B) Western blotting and RT-qPCR detected the expression of PDE2 after cell transfection in OGD/R induced SH-SY5Y cells. (C) RT-qPCR detected the expression of TNF-α, IL-1β, IL-6 and MCP-1. (D) Western blotting was used to detect the expression of p-P65, p-IkB-α, P65 and IkB-α. *P<0.05, **P<0.01, ***P<0.001. PDE, phosphodiesterase; OGD/R, oxygen-glucose deprivation and reoxygenation; RT-qPCR, reverse transcription-quantitative PCR; TNF, tumor necrosis factor; IL, interleukin; MCP, monocyte chemoattractant protein; Iba, ionized calcium binding adaptor; IF, Immunofluorescence; p-, phosphorylated; IkB-α, NF-κB inhibitor α.

was identified in the control group mice. By contrast, cerebral ischemia in the MCAO group was found to be more extensive compared with that in the control group. However, following

administration of Bay-607550 to the model mice, the extent of cerebral ischemic damage was found to be significantly ameliorated (Fig. 2B).
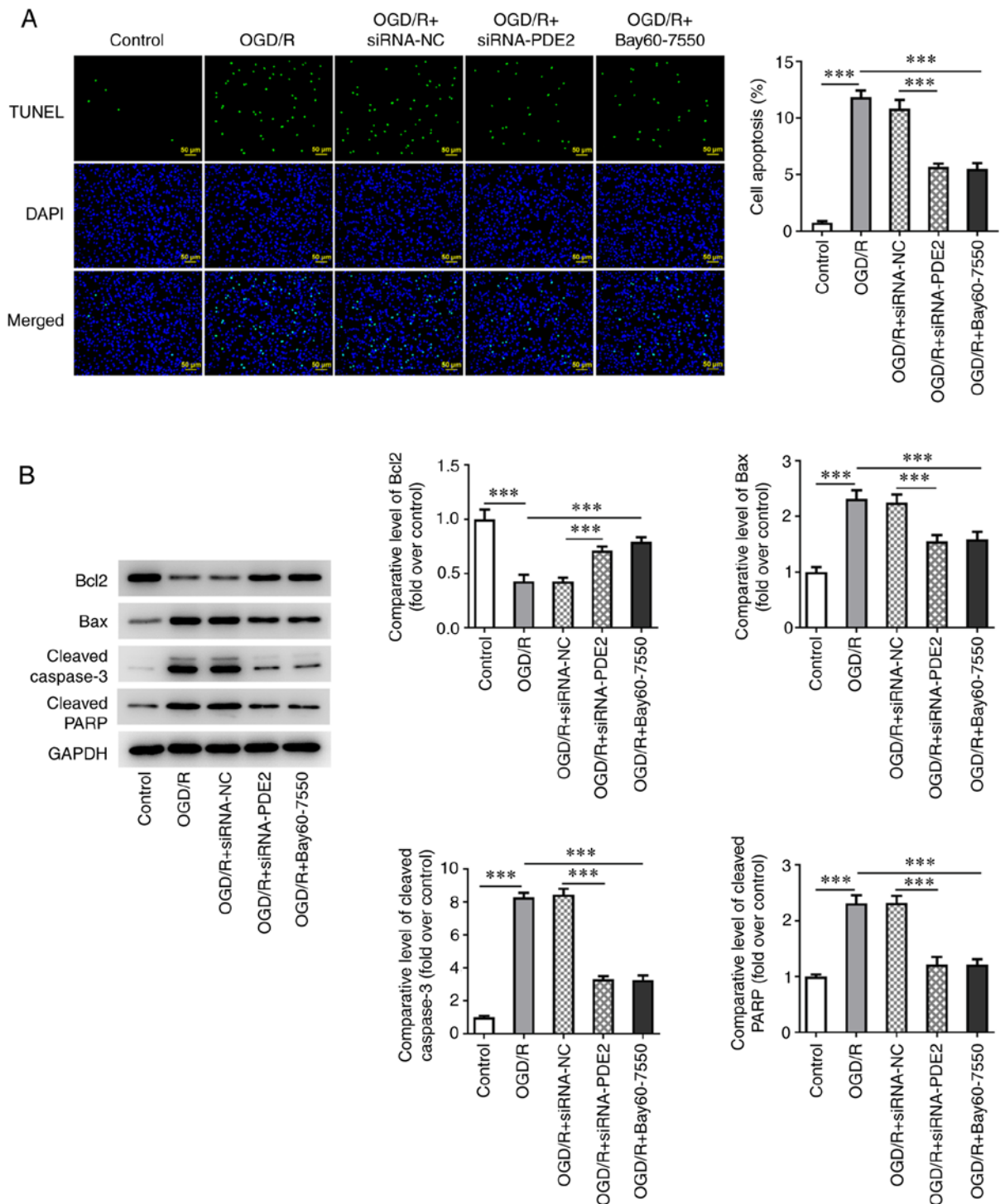
Figure 6. PDE2 inhibitor reduced OGD/R induced neuronal apoptosis. (A) TUNEL assay detected the apoptosis of OGD/R induced SH-SY5Y cells. (B) Western blotting was used to detect the expression of apoptosis related proteins in OGD/R induced SH-SY5Y cells. ***P<0.001. PDE, phosphodiesterase; OGD/R, oxygen-glucose deprivation and reoxygenation.

The PDE2 inhibitor Bay-607550 reduces inflammation and the activation of microglia in CIRI mice. Subsequently, RT-qPCR was used to detect the expression of inflammatory factors in the ischemic site of mice. These experiments showed that the expression levels of tumor necrosis factor-α (TNF-α), interleukin (IL)-1β, IL-6 and monocyte chemoattractant protein-1 (MCP-1) were significantly increased in the MCAO model mice compared with the control group. Compared with the MCAO group, the levels of TNF-α, IL-1β,

IL-6 and MCP-1 were markedly inhibited in the MCAO + Bay-607550 group (Fig. 3A). IF staining, western blotting and RT-qPCR experiments were subsequently used to detect the expression of ionized calcium binding adaptor molecule 1 (Iba-1), a marker of microglia activation and these results showed that, compared with the control group, the expression of Iba-1 in the MCAO group was significantly increased. However, compared with the MCAO group, the expression of Iba-1 was significantly inhibited following Bay-607550

administration (Fig. 3B and C). Subsequently, western blot analysis was used to detect the protein expression levels of the inflammation-associated proteins P65, phosphorylated (p)-P65, NF-κB inhibitor α (IkB-α) and p-IkB-α in cells. These experiments showed that the trends in the alterations of the expression trends of these proteins were consistent with those of the inflammatory factors TNF-α, IL-1β, IL-6 and MCP-1 (Fig. 3D).

The PDE2 inhibitor Bay-607550 reduces the apoptosis of nerve cells in CIRI mice. Finally, the effects of the PDE2 inhibitor Bay-607550 were investigated in a series of *in vivo* animal experiments, The extent of apoptosis was determined in the nerve cells of the mouse brain tissue. The TUNEL assay and western blotting results showed that, compared with the control group, the level of apoptosis was significantly increased in the MCAO group, as shown by the increased expression levels of Bax, cleaved caspase-3 and cleaved poly (ADP-ribose) polymerase (PARP) and a decrease in Bcl-2 expression. Compared with the MCAO group, administration of Bay-607550 led to a significant reduction in the levels of apoptosis observed in the nerve cells, accompanied by decreased expression levels of Bax, cleaved caspase-3 and cleaved PARP and an increase in Bcl-2 expression (Fig. 4A and B).

The PDE2 inhibitor Bay-607550 reduces OGD/R-induced neuronal inflammation and apoptosis. In the cell experiments, SH-SY5Y neurons were selected and the OGD/R model was established. As shown in Fig. 5A, the expression levels of PDE2 were increased in a time-dependent manner as the induction time of OGD/R was increased (Fig. 5A). Since the increases in PDE2 levels were the most marked when the OGD/R model was induced for 24 h, this time point was selected for subsequent experiments. After cell transfection was performed to inhibit the expression levels of PDE2 in the cells, the inhibitory effect of siRNA-PDE2-1, as detected by RT-qPCR and western blot experiments, was found to be the most significant; therefore, siRNA-PDE2-1 was selected as the interfering plasmid of choice for the subsequent experiments (Fig. 5B). The cells were divided into control, OGD/R, OGD/R + siRNA-NC, OGD/R + siRNA-PDE2-1 and OGD/R + Bay607550 groups. The RT-qPCR and western blotting results showed that, compared with the control group, the expression of TNF-α, IL-1β, IL-6, MCP-1 and p-P65 and p-IKBα were significantly increased after OGD/R induction. Compared with the OGD/R group, the expression levels of TNF-α, IL-1β, IL-6, MCP-1 and p-P65 and p-IKBα were significantly inhibited in the OGD/R + Bay-607550 group. Compared with the OGD/R group at 24 h with siRNA-NC treatment, the expression levels of TNF-α, IL-1β, IL-6, MCP-1 and p-P65 and p-IKBα were inhibited in the OGD/R + siRNA-PDE2-1 group (Fig. 5C and D). Subsequently, the apoptotic levels of the cells were detected and the results of the TUNEL assay and western blotting experiments showed that, compared with the control group, the level of apoptosis was significantly increased, as assessed from the significant increases in expression of Bax, cleaved caspase-3 and cleaved PARP in the OGD/R group and marked decrease in Bcl-2 expression. By contrast, compared with the OGD/R group, apoptosis was inhibited, the expression levels of Bax, cleaved caspase-3 and cleaved PARP were
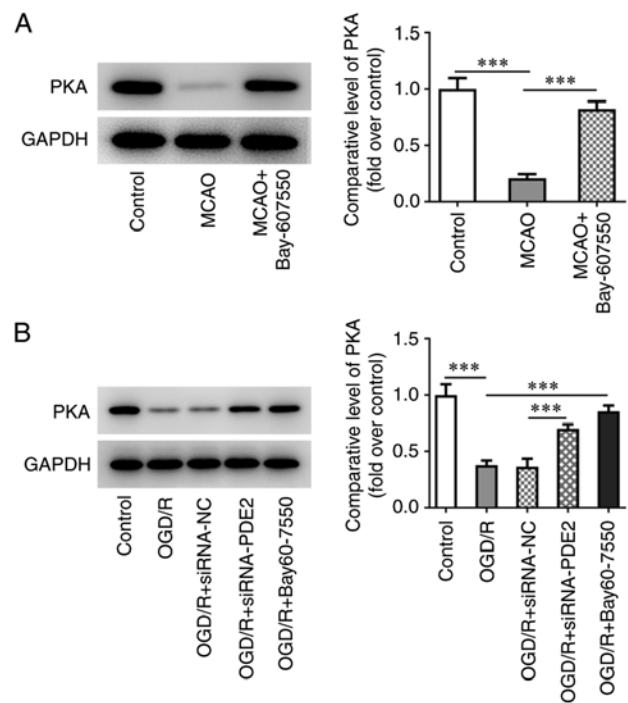

Figure 7. PDE2 inhibitor activated the expression of PKA *in vivo* and *in vitro* in CIRI. Western blot was used to detected the expression of PKA *in vivo* (A) and *in vitro* (B). ***P<0.001. PDE, phosphodiesterase; PKA, protein kinase A; CIRI, cerebral ischemia-reperfusion injury.

decreased and that of Bcl-2 was increased in OGD/R-induced cells that were treated with Bay60-7550. Finally, compared with the OGD/R + siRNA-NC group, the extent of apoptosis was also inhibited in the OGD/R + siRNA-PDE2-1 group, which exhibited decreased expression levels of cleaved caspase-3 and cleaved PARP and an increased expression of Bcl-2 (Fig. 6A and B).

The PDE2 inhibitor Bay-607550 activates the expression of protein kinase A (PKA) both in vivo and in vitro in CIRI mice. In the animal experiments, it was found that, compared with the control group, the expression of PKA in ischemia-reperfusion tissues in the MCAO group was significantly decreased. However, after further administration of Bay-607550, the change in expression level of PKA was found to be reversed (Fig. 7A). Subsequently, western blot analysis was used to detect the expression of PKA in *in vitro* experiments. The results of these experiments showed that, compared with the control group, the expression of PKA in the OGD/R group was significantly decreased, whereas the observed change in PKA expression was reversed in the OGD/R-induced Bay-607550 cells. Furthermore, the expression level of PKA in the OGD/R + siRNA-PDE2 group was also significantly increased compared with the OGD/R + siRNA-NC group (Fig. 7B).

Discussion

The pathophysiological changes associated with nerve injury in CIRI have yet to be fully understood and are currently irreversible; therefore, it is of great value to identify therapeutic targets that could effectively protect patients from the nerve injury that results from reperfusion. The present study has exploited the

fact that abnormal expression of PDE2 is known to be closely associated with the occurrence and development of CIRI (11).

Members of the PDE family are involved in numerous physiological processes in organisms (13,14). A previously published study showed that the PDE4 inhibitor Roflilast prevents ischemic stroke-induced neuronal injury by inhibiting glycogen synthase kinase 3β-mediated oxidative stress and the IRE1α/TRAF2/JNK pathway (15). PDE5 inhibitors inhibit microglia activation and release of inflammatory factors during CIRI (16). K-134 is a PDE3 inhibitor that prevents brain injury via inhibiting thrombosis in a rat cerebral infarction model (17). In addition, PDE7 inhibitors ameliorate brain injury and neuroinflammation during CIRI (18). However, to the to the best of the authors' knowledge, the role of PDE2 in CIRI has yet to be studied in any great depth. In addition, a previous study showed that, following the change in phenotype of the microglia in neural tissues, the expression of PDE2 in the cells change significantly and this phenomenon serves an important role in brain function (19). Sildenafil, a PDE2 inhibitor, inhibits nerve cell apoptosis and inflammation in Alzheimer's disease (20). Therefore, an investigation of the role of PDE2 in CIRI came to be the focal point of the present study. The expression of PDE2 was found to be significantly decreased in MCAO mice and OGD/R-induced neurons. The PDE2 inhibitor Bay-607550 was shown to significantly inhibit brain tissue damage in CIRI-modeled mice, inhibit microglia activation and ameliorate the damaged caused by brain tissue ischemia in mice. The present study only focused on the cerebral ischemia area and did not make as much observation on the penumbra. Special attention will be paid to penumbra in future experiments related to cerebral ischemia.

Possible mechanisms of CIRI include, among other possibilities, the inflammatory response, oxidative stress, intracellular calcium overload, apoptosis and a decreased secretion of neurotrophic factors (21). The early manifestations of CIRI include free radical production, mitochondrial dysfunction, enhanced inflammatory response and neuronal apoptosis, among which neuroinflammation and neuronal apoptosis are the non-negligible causes of CIRI (22). Therefore, the present study focused on the specific role and influence of PDE2 regulation on the inflammatory response and neuronal apoptosis in CIRI disease. The PDE2 inhibitor Bay-607550 was found to inhibit the inflammatory response and apoptosis of neurons in CIRI.

A previous study showed that PDE2 exerts a role through PKA signaling, activating the expression of PKA after PDE2 inhibition (9). Activation of PKA in the peri-ischemic area has an important neuroprotective role in ischemic stroke models (23). Activation of PKA is also shown to reduce neuronal inflammation and apoptosis during CIRI (24). Moreover, PKA can simultaneously affect NF-κB-mediated regulation of inflammation and apoptosis (25). Therefore, a further goal of the present study was to explore whether PDE2 inhibition could activate the expression of PKA signaling protein. It was shown that the PDE2 inhibitor Bay60-7550 could significantly promote the expression of PKA in a CIRI model. In addition, inhibition of PDE2 expression in OGD/R-induced cells significantly promoted the expression of PKA. Therefore, it was possible to tentatively conclude that PDE2 may regulate the inflammatory response and apoptosis

in CIRI through regulating the expression of PKA2. It is aimed to further explore and verify the underlying mechanism in future studies.

Collectively, results of the present study demonstrated that inhibition of PDE2 could reduce inflammation and apoptosis during CIRI through regulating PKA. These findings have provided a basis both for understanding the underlying mechanism of CIRI and for the development of targeted therapies for CIRI in the clinic.

Availability of data and materials

The analyzed data sets generated during the present study are available from the corresponding author on reasonable request.

Authors' contributions

DW, JF and PW designed the study. DW, XW, JF, PW and HX performed the experiments. JF and PW revised the manuscript for important intellectual content. DW, XW and HX collected the clinical data and analyzed the data. DW, XW and HX confirm the authenticity of all the raw data. All authors have read and approved the final manuscript.

Ethics approval and consent to participate

All animal procedures were operated according with the NIH Guide for the Care and Use of Laboratory Animals approved by the ethical guidelines of Wuxi Higher Health Vocational Technology School.

Patient consent for publication

Not applicable.

Competing interests

The authors declare that they have no competing interests.

References

1. Shin TH, Lee DY, Basith S, Manavalan B, Paik MJ, Rybinnik I, Mouradian MM, Ahn JH and Lee G: Metabolome changes in cerebral ischemia. Cells 9: 1630, 2020.
2. Wang H, Chen S, Zhang Y, Xu H and Sun H: Electroacupuncture ameliorates neuronal injury by Pink1/Parkin-mediated mitophagy clearance in cerebral ischemia-reperfusion. Nitric Oxide 91: 23-34, 2019.
3. Wu MY, Yiang GT, Liao WT, Tsai AP, Cheng YL, Cheng PW, Li CY and Li CJ: Current mechanistic concepts in ischemia and reperfusion injury. Cell Physiol Biochem 46: 1650-1667, 2018.
4. Weber S, Zeller M, Guan K, Wunder F, Wagner M and El-Armouche A: PDE2 at the crossway between cAMP and cGMP signalling in the heart. Cell Signal 38: 76-84, 2017.

5. He Y, Huang Y, Mai C, Pan H, Luo HB, Liu L and Xie Y: The immunomodulatory role of PDEs inhibitors in immune cells: Therapeutic implication in rheumatoid arthritis. Pharmacol Res 161: 105134, 2020.
6. Maurice DH, Ke H, Ahmad F, Wang Y, Chung J and Manganiello VC: Advances in targeting cyclic nucleotide phosphodiesterases. Nat Rev Drug Discov 13: 290-314, 2014.
7. Sadek MS, Cachorro E, El-Armouche A and Kämmerer S: Therapeutic implications for PDE2 and cGMP/cAMP mediated crosstalk in cardiovascular diseases. Int J Mol Sci 21: 7462, 2020.
8. Zhou Y, Li J, Yuan H, Su R, Huang Y, Huang Y, Li Z, Wu Y, Luo H, Zhang C and Huang L: Design, synthesis, and evaluation of dihydropyranopyrazole derivatives as novel PDE2 inhibitors for the treatment of Alzheimer's disease. Molecules 26: 3034, 2021.
9. Chen L, Liu K, Wang Y, Liu N, Yao M, Hu J, Wang G, Sun Y and Pan J: Phosphodiesterase-2 inhibitor reverses post-traumatic stress induced fear memory deficits and behavioral changes via cAMP/cGMP pathway. Eur J Pharmacol 891: 173768, 2021.
10. Ruan L, Du K, Tao M, Shan C, Ye R, Tang Y, Pan H, Lv J, Zhang M and Pan J: Phosphodiesterase-2 inhibitor bay 60-7550 ameliorates abeta-induced cognitive and memory impairment via regulation of the HPA axis. Front Cell Neurosci 13: 432, 2019.
11. Soares LM, Meyer E, Milani H, Steinbusch HW, Prickaerts J and de Oliveira RM: The phosphodiesterase type 2 inhibitor BAY 60-7550 reverses functional impairments induced by brain ischemia by decreasing hippocampal neurodegeneration and enhancing hippocampal neuronal plasticity. Eur J Neurosci 45: 510-520, 2017.
12. Livak KJ and Schmittgen TD: Analysis of relative gene expression data using real-time quantitative PCR and the 2(-Delta Delta C(T)) method. Methods 25: 402-408, 2001.
13. Kokkonen K and Kass DA: Nanodomain regulation of cardiac cyclic nucleotide signaling by phosphodiesterases. Annu Rev Pharmacol Toxicol 57: 455-479, 2017.
14. Francis SH, Blount MA and Corbin JD: Mammalian cyclic nucleotide phosphodiesterases: Molecular mechanisms and physiological functions. Physiol Rev 91: 651-690, 2011.
15. Xu B, Xu J, Cai N, Li M, Liu L, Qin Y, Li X and Wang H: Roflumilast prevents ischemic stroke-induced neuronal damage by restricting GSK3beta-mediated oxidative stress and IRE1alpha/TRAF2/JNK pathway. Free Radic Biol Med 163: 281-296, 2021.
16. Moretti R, Leger PL, Besson VC, Csaba Z, Pansiot J, Di Criscio L, Gentili A, Titomanlio L, Bonnin P, Baud O and Charriaut-Marlangue C: Sildenafil, a cyclic GMP phosphodiesterase inhibitor, induces microglial modulation after focal ischemia in the neonatal mouse brain. J Neuroinflammation 13: 95, 2016.
17. Yoshida H, Ashikawa Y, Itoh S, Nakagawa T, Asanuma A, Tanabe S, Inoue Y and Hidaka H: K-134, a phosphodiesterase 3 inhibitor, prevents brain damage by inhibiting thrombus formation in a rat cerebral infarction model. PLoS One 7: e46432, 2012.
18. Redondo M, Zarruk JG, Ceballos P, Pérez DI, Pérez C, Perez-Castillo A, Moro MA, Brea J, Val C, Cadavid MI, et al: Neuroprotective efficacy of quinazoline type phosphodiesterase 7 inhibitors in cellular cultures and experimental stroke model. Eur J Med Chem 47: 175-185, 2012.
19. Bender AT and Beavo JA: Specific localized expression of cGMP PDEs in Purkinje neurons and macrophages. Neurochem Int 45: 853-857, 2004.
20. Sanders O: Sildenafil for the treatment of Alzheimer's disease: A systematic review. J Alzheimers Dis Rep 4: 91-106, 2020.
21. Orellana-Urzua S, Rojas I, Libano L and Rodrigo R: Pathophysiology of ischemic stroke: Role of oxidative stress. Curr Pharm Des 26: 4246-4260, 2020.
22. Polderman KH: Mechanisms of action, physiological effects, and complications of hypothermia. Crit Care Med 37: S186-S202, 2009.
23. Li H, Wang J, Wang P, Rao Y and Chen L: Resveratrol reverses the synaptic plasticity deficits in a chronic cerebral hypoperfusion rat model. J Stroke Cerebrovasc Dis 25: 122-128, 2016.
24. Liu Y, Zhang J, Zan J, Zhang F, Liu G and Wu A: Lidocaine improves cerebral ischemia-reperfusion injury in rats through cAMP/PKA signaling pathway. Exp Ther Med 20: 495-499, 2020.
25. Hu X, Li S, Doycheva DM, Huang L, Lenahan C, Liu R, Huang J, Gao L, Tang J, Zuo G and Zhang JH: Rh-CSF1 attenuates oxidative stress and neuronal apoptosis via the CSF1R/PLCG2/PKA/UCP2 signaling pathway in a rat model of neonatal HIE. Oxid Med Cell Longev 2020: 6801587, 2020.